Available online at www.sciencedirect.com

ScienceDirect

Vision Research 48 (2008) 127–135

Vision Research

www.elsevier.com/locate/visres

Retinal and cortical patterns of spatial anisotropy in contrast sensitivity tasks

Maria Fatima Silva, Susana Maia-Lopes, Catarina Mateus, Manuela Guerreiro, Joana Sampaio, Pedro Faria, Miguel Castelo-Branco *

Centre for Opthalmology, Visual Neuroscience Laboratory, IBILI, Faculty of Medicine, Az. de Sta Comba, 3000-354 Coimbra, Portugal

Received 8 June 2007; received in revised form 19 October 2007

Abstract

It has often been postulated that asymmetries in performance within the visual field (VF) are not characteristic of early visual processing. Here, human retinal (naso/temporal), cortical (left/right) and superior/inferior patterns of asymmetry were explored with achromatic contrast sensitivity (CS) tasks, that probed distinct spatiotemporal frequency channels. Low spatial, high temporal frequency stimuli (illusory frequency-doubling (FD)) yielded superior and temporal field disadvantage. Independent right and nasal visual hemifield patterns of disadvantage were found when probing an intermediate spatial frequency (ISF) channel, with stationary sinusoidal gratings. These findings show that asymmetries in spatial vision are explained by independent retinal and cortical mechanisms.

Keywords: Contrast sensitivity; Asymmetry; Spatial vision; Magnification factor; Visual system; Cerebral dominance; Hemispheric specialization

1. Introduction

Psychophysical performance has often been assumed to be symmetric in terms of early level visual function, although visual field (VF)[1] asymmetries have been established for higher level psychophysical tasks (Edgar & Smith, 1990; Hugdahl & Davidson, 2003; Ivry & Robertson, 1998; Nakayama & Mackeben, 1989; Previc, 1990; Rubin, Nakayama, & Shapley, 1996). This is quite surprising, given the available anatomical and physiological data for anisotropies in early visual pathways including cortical retinotopic areas and the retina (see below).

Some recent studies have emphasized the ecological relevance of dorso/ventral anisotropies (above and below the horizon) and focused on cardinal visual meridians, raising the question whether asymmetries in letter identification (Mackeben, 1999), visual acuity (Altpeter, Mackeben, & Trauzettel-Klosinski, 2000) and attentional conjunctive visual search tasks (He, Cavanagh, & Intrilligator, 1996), generalize to other VF locations. An early cortical contribution to asymmetric visual performance has also been recently considered (Carrasco, Talgar, & Cameron, 2001; Carrasco, Giordano, & McElree, 2004) independently of attentional biases. A retinal contribution was however not isolated and separately investigated in these studies (Carrasco et al., 2001, 2004), because performance was analyzed only under binocular conditions. This fact precluded the possibility of exploring naso/temporal biases, which could provide direct evidence for independent retinal mechanisms underlying functional asymmetries. Retinal naso/temporal asymmetries are indeed canceled out within left/right cortical binocular representations, due to the normal crossing of visual pathways (for instance, the left hemifield corresponds to the nasal retina of the left eye and the temporal retina of the right eye), and this fact was also not taken into account in earlier studies using CS tasks (Rijs-

* Corresponding author. Fax: +351 239 480 280.
E-mail address: mcbranco@ibili.uc.pt (M. Castelo-Branco).

[1] *Abbreviations used:* VF, visual field; CS, contrast sensitivity; FD, frequency-doubling; cpd, cycles per degree; ISF, intermediate spatial frequency; LSF, low spatial frequency; OS, left eye; OD, right eye; P, parvocellular; M, magnocellular; ISI, interstimulus interval; IN, inferonasal; IT, inferotemporal; SN, superonasal; ST, superotemporal.

0042-6989/$ - see front matter © 2007 Elsevier Ltd. All rights reserved.
doi:10.1016/j.visres.2007.10.018

dijk, Kroon, & van der Wilt, 1980; Rovamo & Virsu, 1979). Previous studies have however noted a possible role for naso/temporal asymmetries in CS in particular in hyper acuity tasks (Fahle & Schmid, 1988).

Previous anatomical findings suggest a possible neural basis for performance anisotropies of retinal origin. Differences in cell density can be related to relative magnification factors (M-scaling, e.g., mm of cortical surface per degree of visual space) of visual representations (Myerson, Manis, Miezin, & Allman, 1977; Van Essen, Newsome, & Maunsell, 1984; Virsu & Rovamo, 1979) and have been well documented in many species (Andrade da Costa & Hokoc, 2000; Chandler, Smith, Samuelson, & MacKay, 1999; Kryger, Galli-Resta, Jacobs, & Reese, 1998; Packer, Hendrickson, & Curcio, 1989; Perry & Cowey, 1985; Wikler & Rakic, 1990a; Wikler, Williams, & Rakic, 1990b), including the human eye (Curcio & Allen, 1990a; Curcio, Sloan, Kalina, & Hendrickson, 1990b; Østerberg, 1935). It is also well established that differences in cell density can explain differences in visual performance (Drasdo, 1977; Levi, Klein, & Aitsebaomo, 1985; Rolls & Cowey, 1970; Rovamo, Virsu, & Nasanen, 1978; Schein, 1988; Thibos, Cheney, & Walsh, 1987; Weymouth, 1958; Williams & Coletta, 1987). All of these studies are consistent with strong naso/temporal biases: cone and ganglion cell densities are larger in the nasal retina (temporal VF) and these anisotropies in neural representations are further propagated to subsequent processing streams (Connolly & Van Essen, 1984; Van Essen et al., 1984). These anatomical asymmetries are also consistent with well documented electrophysiological data in humans (Marmor et al., 2003).

In the present study, we aimed to investigate early level visual asymmetries by measuring achromatic CS under conditions that activate two distinct spatiotemporal frequency channels. To assess a LSF (low spatial frequency) channel we used a CS detection task which employs a low spatial frequency (0.25 cpd) grating counterphasing at 25 Hz which elicits a characteristic FD illusion. This condition has probably some selectivity for the M (magnocellular) system, which is generally more sensitive to high temporal and low spatial frequencies, in contrast to the P system, that is more sensitive to stimuli with low temporal and high spatial frequencies (Lee, Martin, Valberg, & Kremers, 1993; see also Silva et al., 2005, and references therein).

To explore an ISF (intermediate spatial frequency) channel we used static sinusoidal gratings of intermediate spatial frequency (3.5 cpd). This spatial frequency only provides relative isolation (mixed *P*-test), in particular in central VF locations. That spatial frequency is however relatively high for more peripheral locations (beyond central 5°), which were the focus of our analyses of CS asymmetries. All of our low level visual CS tasks were performed with conditions that keep attention homogeneously distributed over the VF, by running randomly interleaved staircases in space and time, in order to unravel separate retinal and cortical mechanisms underlying anisotropies in spatial vision.

The main goal of this study was therefore to test for the presence of asymmetries in low level visual CS tasks in terms of left/right (interhemispheric), superior/inferior, and nasal/temporal (retinal) hemifields, concerning distinct spatiotemporal frequency channels. We took into account in our approach the interaction between different types of asymmetry. For example right/left anisotropies should interact with naso/temporal asymmetries in an eye-dependent manner: in case of putative temporal and left field advantages, effects should summate for the left eye, because they coincide, and cancel out for the right eye. This study separates for the first time retinal and cortical mechanisms underlying psychophysical anisotropies, and shows that they are distinct in temporal and spatial vision.

2. Methods

2.1. Participants

A complete neuro-ophthalmological examination was performed in all individuals by two ophthalmologists (LD and author PF). This exam consisted of best-corrected visual acuity (VA—Snellen chart), IOP measurement (Goldman applanation tonometer), slit lamp examination of anterior chamber, angle and fundus examination (Goldman lens). Exclusion criteria included the following: pseudophakic and aphakic eyes, cataract or other eye disease that might interfere with fundus examination, retinal diseases, neuro-ophthalmologic pathology, and high ammetropia (sphere dpt > 4 and cylinder dpt > 2).

Subject distribution for the ISF task, was as follows: $n = 18$ subjects (36 eyes; 8 male, 10 female) with mean age of 25 ± 3 years (mean $\pm$ SD) for monocular testing and $n = 18$ for the binocular condition. Regarding the two approaches used for LSF perimetry (our own custom approach; and FD commercially available Humphrey Matrix N-30-*F* test strategy; for details see below), age distributions were as follows: mean age of 33 ± 10 years for $n = 48$ subjects (88 eyes; 23 male, 25 female subjects) for the latter strategy; and concerning the custom approach, mean age of 27 ± 4 years for $n = 20$ subjects (36 eyes; 8 male, 12 female subjects). Thirteen subjects performed both LSF tests.

Informed consent was obtained from all participants. The study was conducted in accordance with the tenets of the Declaration of Helsinki, and with the guidelines of the Ethics Committee of the Faculty of Medicine of Coimbra. In this study all subjects were right-handed and naive to the purpose of the tests performed, and had normal or corrected-to-normal visual acuity.

2.2. Intermediate spatial frequency (ISF) contrast sensitivity test

In the CS detection task that was used to assess the ISF channel, stimuli were patches of vertically oriented sinusoidal gratings, with a spatial frequency of 3.5 cpd and 0 Hz temporal frequency (mean background luminance of 51 cd/m^2), displayed on a gamma corrected 21 inch. Trinitron GDM–F520 Sony color monitor (frame rate 100 Hz) at a viewing distance of 36 cm. The test was generated from a CRS/VSG 2/5 graphics card (Cambridge Research Systems, [CRS], Rochester, UK), using the CRS object animation library) (Silva et al., 2005). Standard voltage–luminance curves were measured for each phosphor with software and hardware (including a Minolta colorimeter) provided by CRS, which ensured gamma correction. Luminance contrast modulation of the stimuli was expressed according to Michelson luminance contrast $(\%) = 100 * (L_{max} - L_{min})/(L_{max} + L_{min})$. An adaptive logarithmic staircase strategy was used to obtain psychophysical thresholds. The value to be used for a given trial was calculated using the previous trial value plus or minus the step size in dB. The initial step size used was 3 dB. Staircases were

run for a total of four reversals, with the contrast at the final two reversals being averaged to estimate the contrast threshold. The results were expressed in terms of decibels (dB) units, $dB = 20 * \log(1/c)$, with contrast c measured as a percentage.

The stimulus was used as a detection target and presented pseudo-randomly within 9 locations, (see top inset of Fig. 1, perimetry field divided into three zones): zone 0 corresponds to a 5° central visual region (C), zone 1 includes stimuli between 5° and 10° eccentricity and zone 2 contains stimuli between 10° and 20° eccentricity. Subjects were instructed to fixate the black square (1° × 1°) in the center of the screen and report the presence of "striped" targets (see top inset in Fig. 1) by means of a button press. Stimulus duration was 200 ms and ISI was jittered between 2300 and 2800 ms. Participants' reliability was evaluated by randomly interleaving False positive (with 0% contrast stimuli) and negative (100% contrast) catch trials. We excluded all results with false positive and false negative errors ⩾33%, according to standard criteria (Caprioli, 1991). Fixation loss was monitored with our custom eye-tracking methodology (CRS device) which provides detailed measurements of eye position. This perimetric task was performed in a monocular way for both eyes, with the first tested eye being chosen in a random manner (an opaque black patch was used to occlude the non-tested eye). The task was also performed under binocular conditions, to replicate the left/right asymmetry observed under monocular conditions.

2.3. Low spatial frequency (LSF) contrast sensitivity test–FD test

Our LSF stimuli had spatiotemporal properties that induce a well known illusory FD (frequency doubling) of the number of perceived stripes (see Silva et al., 2005 and references therein). FD–CS was measured in two different ways, one using custom software and CRS hardware (Mendes et al., 2005; Silva et al., 2005) and a commercially available system (Humphrey Matrix perimeter, Welch Allyn, Skaneateles, NY; Zeiss–Humphrey, Dublin, CA). In all CS detection target strategies, stimuli were patches of 0.25 cpd vertically oriented sinusoidal gratings, undergoing 25 Hz counterphase flicker.

Implementation, calibration, stimulus geometry, test strategy and performance reliability in our custom approach was identical to the one described in the previous section except when otherwise stated. We have tested two sets of background luminances (61.7 and 100 cd/m^2 for the custom and standard LSF approaches, respectively). For the standard device we used a strategy (N-30-F) which tests a total of 17 locations (four 10° diameter square targets per quadrant and a central 5° radius circular target) plus 2 nasal locations (the horizontal area tested is extended to include an extra portion of the nasal VF, resulting in a total 30° horizontal field). The threshold strategy is known as Modified Binary Search (MOBS) with a dynamic luminance ratio range from 56 to 0 dB. Stimulus duration was 300 ms. Performance reliability was assessed by monitoring fixation loss with the Heijl–Krakau method (Caprioli, 1991), and by computing false positive and negative errors. We have found 2.3% fixation errors using this method and exclusions were made according to the standard criteria described in the previous section. As in the ISF experiment, subjects were instructed to fixate the black square in the center of the screen and report the presence of "striped" targets. All participants performed the tests under monocular conditions and the first tested eye was chosen in a random manner. Since no left/right asymmetry was observed under monocular conditions, no replication was needed in this case for binocular conditions.

2.4. Statistical analysis

To examine spatial perceptual asymmetries we have used parametric statistics both for pairwise/quadrantwise assessment of VF asymmetries (paired t-test when analyzing hemifield patterns of asymmetry and/or repeated measures ANOVA for quadrantwise analyses), after verifying that the data did not significantly deviate from normal distributions. The central 5° region of higher CS was excluded in all data analyses of spatial asymmetries, since it gives a homogeneous contribution for all quadrants and hemifields, and is therefore irrelevant to the analysis of anisotropy. Note that for the LSF testing condition, 9 locations were tested in the custom approach as compared to 17 locations (9 of which matching exactly the ones used in the custom approach) in the standard method (2 additional nasal locations were excluded so that comparisons between both approaches were made in matched locations within the same range of eccentricity, 20°). Statistical analysis was done with the STATVIEW and SPSS software packages (SAS, Cary, NC and SPSS, Inc., Chicago, IL, respectively).

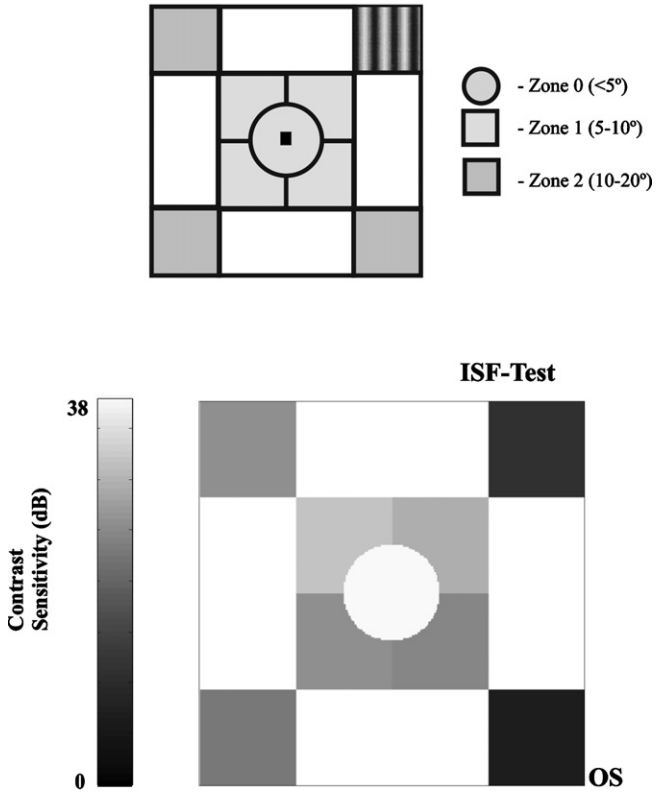

Fig. 1. Top inset: basic scheme of VF locations, tested in the custom approach (in a pseudorandomly interleaved manner). All 17 locations plus 2 positions in the nasal field were tested in the LSF standard task (the 9 locations tested in the custom approach matched 9/17 locations tested in the standard approach). Sinusoidal gratings were used as detection target stimuli for all tasks (for details see Section 2). Lower panel: gray scale CS map for ISF stimuli tested in 9 locations, depicted from a subject with strong asymmetry (due to synergistic summation of left/right and nasotemporal asymmetries in left monocular testing – for details see Text). Darker regions correspond to areas of lower CS (the central region is very bright due to very high contrast sensitivity).

3. Results

3.1. Naso/temporal VF asymmetries in the ISF task

Measurements of monocular CS across the VF with the ISF (intermediate spatial frequency) condition showed a mean value of 24.7 ± 6.2 dB which was consistently lower than the ones found for the LSF test conditions (see below and summary in Fig. 6). An individual CS map is illustrated in Fig. 1. The group analysis of hemifield asymmetries (Fig. 2), showed a significant naso/temporal pattern

of VF anisotropy (paired t-test: $p = .0002$; nasal hemifield pattern of disadvantage).

We have also performed analysis split by VF quadrants, because most cortical areas beyond V1 are organized into separate quadrant representations and to further document whether the strength of naso/temporal asymmetries was modulated by a dorso/ventral (up/down) factor. This analysis did confirm, as expected, significant differences in performance across visual quadrants (repeated measures ANOVA with $n = 4$ levels: $p = .001$).

Accordingly, we found predominant IN (inferonasal) and SN (superonasal) field disadvantage (corresponding to supero and inferotemporal retina) in comparison to IT and ST regions. Differences between IN and in particular region IT, were significant ($p < .0001$) even after correction for multiple comparisons.

3.2. Cortical left/right VF asymmetries in the ISF task

A significant cortical hemifield effect (performance in the left hemifield being significantly better than the right hemifield) was found (Fig. 3; paired t-test for left/right hemifield comparisons: $p = .013$). This pattern of cortical left hemifield advantage was further confirmed ($p = .0071$) when considering experiments performed under binocular conditions (Fig. 3).

Hemifield (interhemispheric) performance was then analyzed separately for each eye, to better understand the interaction between naso/temporal field asymmetries (that can better be separated by considering each eye separately) and cortical left/right anisotropies (since the left hemifield includes the nasal VF of OD and the temporal VF of OS). When the analysis of left/right asymmetries was split by eye, significance was found specifically for the OS ($p < .0001$, see Fig. 3). Note in Fig. 3, that the left panel represents data pooled across eyes, but the source of the effect becomes clearer in the right panel. The effect was indeed strongest for the left eye, and binocular conditions. However it was not present or even occasionally reversed for the right eye. This was expected from our interaction hypothesis that the left field advantage should summate with the corresponding temporal VF advantage in OS, and should cancel out with the corresponding nasal VF disadvantage in the OD. If this were the case, a significant interaction between the left/right VF asymmetry and tested eye should be observed. This was indeed the case ($p = .002$, concerning analysis of the interaction between these factors).

3.3. Naso/temporal and dorso/ventral patterns of asymmetry in the LSF task

We have measured monocular CS across the VF, using FD stimuli. Contrast sensitivities were on average slightly higher (Figs. 4–6) when compared with the ISF task, which probed a higher spatial frequency. The similarity of representative CS maps obtained with two distinct LSF approaches can be appreciated in Fig. 4A (standard) and B (custom).

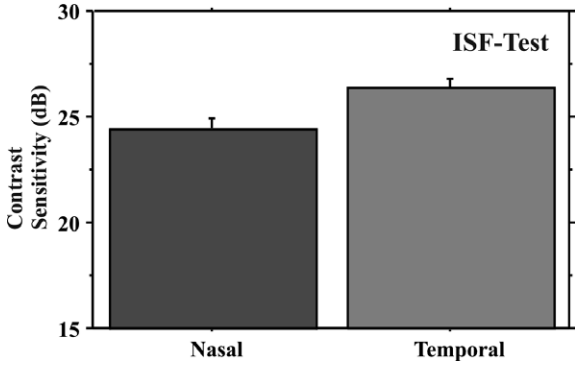

Fig. 2. Comparison of performance in nasal and temporal VF regions, for the ISF task. Error bars correspond to 1 SE of the mean. A naso/temporal pattern of asymmetry (nasal field disadvantage) was found (paired t-test: $p = .0002$).

It is interesting to note that a quadrant-like pattern of asymmetry was found, which is likely due to the combination of naso/temporal and dorso/ventral anisotropies. Indeed, a superior/inferior asymmetry was present (paired t-test: standard method, $p = .0011$ and custom, $p = .0098$; see Fig. 5A) as well as a pattern of naso/temporal anisotropy that however, only reached significance for the standard method (Fig. 5B; standard, $p < .0001$ and custom, $p = .1686$). It is worth noting that the pattern of temporal field disadvantage observed for this task was opposite to the one observed for the ISF task (see Section 4) as would be expected from the fact that distinct stimulus properties tap separate mechanisms. No control binocular tests were done in this case since no left/right bias was found under monocular conditions.

Analyses split by VF quadrants confirmed the ST (superotemporal) pattern of disadvantage (inferior nasal retina) for both LSF probing methods, (Fig. 4, repeated-measures ANOVA, with $n = 4$: standard, $p < .0001$ and custom, $p = .001$; effects remaining significant after correction for multiple comparisons). For the standard approach, differences were significant in particular for post hoc comparisons between ST and all other quadrants ($p < .0001$). In this condition, the higher number of tested locations increased statistical power. In the custom approach, significance was found only between ST and IT ($p < .0001$).

3.4. Center-periphery CS differences across distinct sensory mechanisms

Comparisons of CS for ISF and LSF custom tasks across regions of different eccentricities are plotted in Fig. 6. It is worth noting the relatively flat profile of eccentricity dependence observed for performance in the LSF test when compared with ISF test, suggesting that eccentricity dependence of CS and its relation to M-scaling (mm of cortical surface/°) is less prominent than for the ISF channel. This evidence that the LSF channel has likely

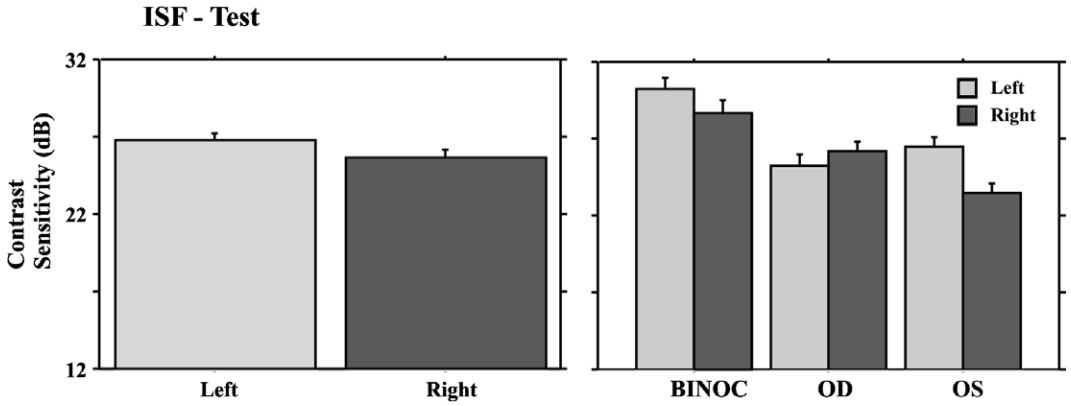

Fig. 3. Left/right hemifield performance asymmetries (of likely cortical origin) were also observed in our ISF test (paired t-test, $p = .013$). When analysis was split by eye, significance was specifically found for OS ($p < .0001$). Binocular (BINOC) testing showed the same pattern of cortical left hemifield advantage ($p = .0071$).

a less steep magnification profile than the pathways related to the ISF channel suggests that if one normalizes the data using the equations described in Virsu and Rovamo (1979) (data not shown) this would have lead to an overestimation of peripheral performance in the LSF task.

4. Discussion

This study demonstrates perceptual anisotropies of low level cortical (left/right) and retinal (naso/temporal) or mixed (dorso/ventral) origin which are distinct within the two tested spatiotemporal frequency channels. Combinations of different types of hemifield asymmetries also yielded quadrant-like patterns of anisotropy.

In our ISF (intermediate spatial frequency) task, we found that retinal mechanisms are modulated by a surprising left hemifield advantage of cortical origin, which was not previously reported for such low level detection tasks (Hugdahl & Davidson, 2003; Ivry & Robertson, 1998). Our experimental design was able to render attention

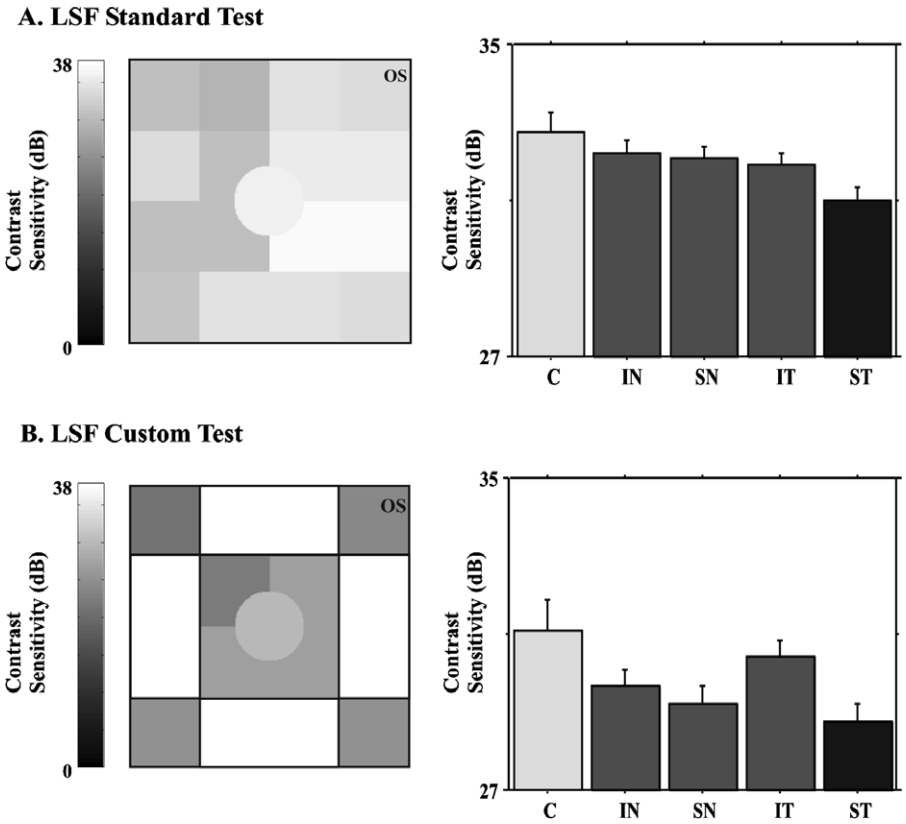

Fig. 4. Left panels: CS maps from OS eyes of representative normal subjects (using standard and custom LSF tests; for details see Section 2). Right panels: bar plots depicting CS for each quadrant: IN, inferonasal; IT, inferotemporal; SN, superonasal; ST, superotemporal; C, central 5° region. For both LSF tests, a ST pattern of disadvantage (inferior nasal retina) was found (see Section 3).

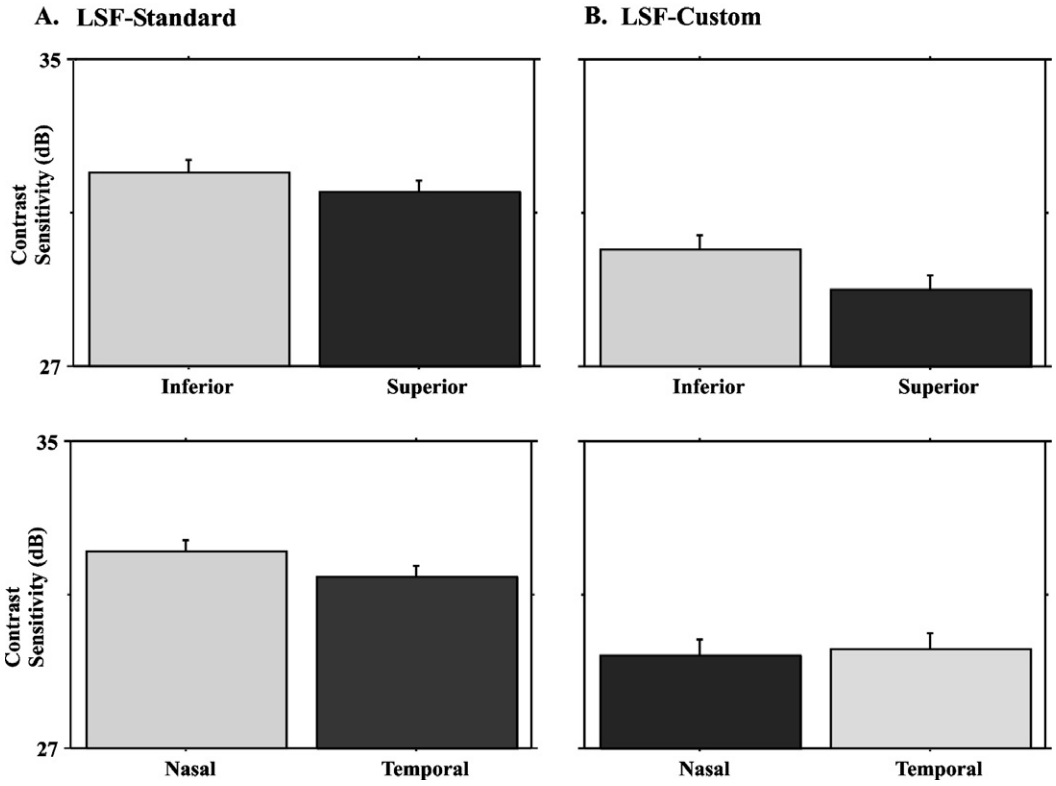

Fig. 5. Naso/temporal and superior/inferior patterns of performance are summarized in bar plots for tests described in Fig. 4. (A) Significant superior/inferior asymmetries were found for both (paired t-test: standard, $p = .0011$ and custom, $p = .0098$). (B) A strong naso/temporal asymmetry (temporal field disadvantage) was found only for standard approach (standard, $p < .0001$). In all figures, darker bars correspond to lower CS.

homogeneous across space, by interlacing tests simultaneously across the VF, thereby rendering stimulus presentation unpredictable. All results (right and nasal hemifield patterns of disadvantage when assessing ISF channel and quadrant-like combined superotemporal pattern of asymmetry for the LSF approach) showed unequivocal evidence for pre-attentive low level visual anisotropies that includes early contrast processing, also contradicting traditional postulates of pure high level asymmetries (Hugdahl & Davidson, 2003; Ivry & Robertson, 1998). Some previous studies were performed under binocular conditions, which precluded analysis of the contribution of low level retinal factors and thereby missing naso/temporal asymmetries (see however the findings of Fahle & Schmid, 1988; Fahle & Wehrhahn, 1991 concerning hyperacuity and motion tasks). Furthermore, we have verified that retinal naso/temporal asymmetries interact significantly with left/right cortical binocular representations (summating, as expected from the anatomical arrangement and monocular psychophysical asymmetry patterns, synergistically for the left eye and antagonistically for the right eye, an effect that is independent of eye dominance). Indeed right/left anisotropies should interact with naso-temporal asymmetries in an eye-dependent manner: in case of temporal and left field advantages, as found, effects should summate for the left eye, because they coincide, and cancel out for the right eye.

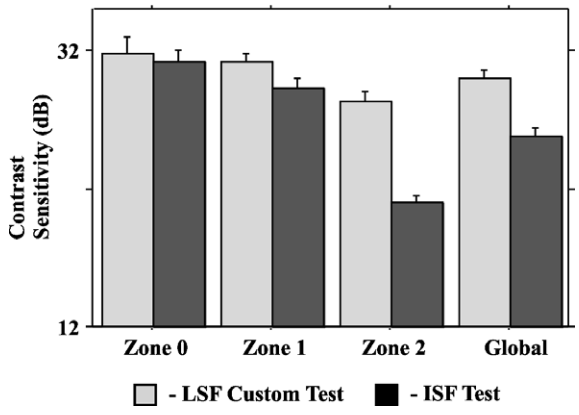

Fig. 6. CS dependence on eccentricity is different for custom ISF and LSF tasks. Zones are as defined in Fig. 1 and "Global" measure corresponds to an average across the three zones. The relatively flat profile observed for the LSF test would predict that classical M-scaling procedures can lead to deviations in correct CS estimation (for details see text).

The temporal disadvantage observed with the LSF task combines with the also observed dorso/ventral asymmetry (inferior field superiority) related with LSF channel, which routes predominantly to the visual dorsal stream. This finding generalizes previous reports suggesting enhanced anatomical representation of the lower VF (Van Essen et al., 1984), with better performance in this region for several tasks (Altpeter et al., 2000; Carrasco, McLean, Katz, & Frieder, 1998; Carrasco et al., 2004; Mackeben, 1999;

Rubin et al., 1996). The superior/inferior asymmetry in the LSF condition mirrors the pattern observed for other tasks. Usually subjects perform better when stimuli are in the inferior visual hemifield. This is not surprising, since ganglion cell densities are higher in the superior retina (Curcio & Allen, 1990a) and the fact that most interesting visual events occur below the line of horizon (Previc, 1990, for review). It is surprising that the magno-biased LSF test gives a pattern of asymmetry opposite to the ISF task. It remains to be explored whether these naso/temporal performance differences observed for LSF tests are related to anatomical asymmetries such as naso/temporal size differences in primate ganglion cell dendritic arborizations (Dacey & Petersen, 1992; Silveira & Perry, 1991; Yamada, Silveira, Perry, & Franco, 2001). This would imply a distinct explanation not based on cell number as was the case for the ISF task. Indeed, Silveira and Perry (1991) noted that M-ganglion cells in the nasal region of the retina (temporal field) have relatively smaller dendritic trees. Dacey and Petersen (1992) have previously correlated larger dendritic field sizes of human parasol cells, with a lower resolving ability and an increased sensitivity to luminance contrast than their equivalents in the macaque. Concerning the different VF field performance observed for the magno task we can therefore speculate that it is likely related to naso-temporal size differences in primate ganglion cell dendritic arborizations. Indeed, temporal ganglion cells tend to have larger dendritic fields than nasal cells (Yamada et al., 2001). Furthermore, P (midget) and M (parasol) ganglion cells in owl monkeys have larger dendritic fields than those of diurnal primates (Silveira, Yamada, Perry, & Picanco–Diniz, 1994; Yamada, Marshak, Silveira, & Casagrande, 1998). The fact that ganglion cells in primates with predominant nocturnal vision (requiring higher CS) have larger dendritic fields than those of diurnal primates further supports the idea that larger dendritic trees may yield better CS. Indeed, larger dendritic trees imply sampling of a larger number of photoreceptors and thereby larger sensitivity (see also the classical evidence for the relation between spatial summation and contrast sensitivity: Shapley, Kaplan, & Soodak, 1981). If this is the case also for the human retina, then this might well represent a neuronal correlate of the higher CS we have observed for that part of the retina.

Concerning the intermediate spatial frequency channel (ISF test), the novel and surprising pattern of left hemifield advantage suggests that an interhemispheric effect can powerfully modulate performance even for low level CS tasks. This extends the previously known right hemispheric dominance for high level spatial vision tasks (Hugdahl & Davidson, 2003) also to early vision mechanisms. This is specifically true for the ISF task which is probably related to the fact that spatial vision mechanisms are more heavily recruited with detailed higher spatial frequency stimuli.

The enhanced nasal VF disadvantage provides direct evidence for an additional retinal mechanism contributing to anisotropic performance, and is consistent with the correspondingly lower cone/ganglion cell density profiles in the temporal retina (Curcio & Allen, 1990a; Curcio et al., 1990b; Dacey, 1993; Drasdo, Millican, Katholi, & Curcio, 2007). Anatomical anisotropies within the retina have been well documented and are consistent with our own optical coherence tomography (data not shown) and multifocal electrophysiology data; see also Marmor et al., 2003.

In sum, the left hemifield advantage observed for the ISF test mirrors the well known right hemisphere specialization in spatial vision, and the nasal field disadvantage may reflect the less stringent need to better resolve that part of the VF under monocular conditions.

The observed differences in VF performance suggest different ecological constraints and that distinct magnification factors should be applied for each spatiotemporal channel. Accordingly, when comparing CS for ISF and LSF custom tasks across regions of different eccentricities we have found that LSF (magno) sensitivities fall off less quickly with increasing eccentricity than their ISF (parvo) sensitivities (on the issue of corresponding parvo/magno anatomical naso-temporal asymmetries at the level of the retina and LGN see Dacey & Petersen, 1992 and Connolly & Van Essen, 1984, respectively).

As discussed above, the distinct CS's found for LSF and ISF test conditions suggest that, the two types of gratings used can provide different activation bias concerning parvo and magnocellular (M) visual pathways. We speculate that ISF condition taps more the peripheral P pathway (at least compared to the magno-like LSF condition). The lower CS observed for the ISF task could possibly reflect the lower ganglion cell convergence within the P pathway (Perry & Cowey, 1985; Yamada et al., 2001). Accordingly, we have observed the expected higher CS at all eccentricities at high temporal frequencies imposed by our M-like LSF task conditions. Furthermore there is also evidence that LSF stimuli favor the M pathway (Derrington & Lennie, 1984; Lee et al., 1993; Maddess et al., 1999).

In conclusion, our findings shed new light on the role of low level spatial vision on functional asymmetries in visual perception. Future studies should further elucidate the relative role of such functional anisotropies in different visual tasks and contexts.

Acknowledgments

We thank PG+Hitec Zeiss, Portugal for technical support, Sandrina Nunes, for advice concerning statistical analysis, and Lillianne Duarte for help in ophthalmological assessment. This work was supported by the following Grants: Bial 15/02, Portugal, POCI_SAU-OBS_57070_2004, and Gulbenkian Foundation/Visual Ageing. M.F.S. and S.M.-L. were supported by individual fellowships from the Portuguese Foundation for Science and Technology (FCT/SFRH/BD/18777/2004, FCT/SFRH/BD/11828/2003).

References

Altpeter, E., Mackeben, M., & Trauzettel-Klosinski, S. (2000). The importance of sustained attention for patients with maculopathies. *Vision Research, 40*, 1539–1547.

Andrade da Costa, B. L., & Hokoc, J. N. (2000). Photoreceptor topography of the retina in the New World monkey Cebus apella. *Vision Research, 40*, 2395–2409.

Caprioli, J. (1991). Automated perimetry in glaucoma. *American Journal of Ophthalmology, 111*, 235–239.

Carrasco, M., McLean, T. L., Katz, S. M., & Frieder, K. S. (1998). Feature asymmetries in visual search: Effects of display duration, target eccentricity, orientation and spatial frequency. *Vision Research, 38*, 347–374.

Carrasco, M., Talgar, C. P., & Cameron, E. L. (2001). Characterizing visual performance fields: Effects of transient covert attention, spatial frequency, eccentricity, task and set size. *Spatial Vision, 15*, 61–75.

Carrasco, M., Giordano, A. M., & McElree, B. (2004). Temporal performance fields: Visual and attentional factors. *Vision Research, 44*, 1351–1365.

Chandler, M. J., Smith, P. J., Samuelson, D. A., & MacKay, E. O. (1999). Photoreceptor density of the domestic pig retina. *Veterinary Ophthalmology, 2*, 179–184.

Connolly, M., & Van Essen, D. (1984). The representation of the visual field in parvocellular and magnocellular layers of the lateral geniculate nucleus in the macaque monkey. *The Journal of Comparative Neurology, 266*, 544–564.

Curcio, C. A., & Allen, K. A. (1990a). Topography of ganglion cells in human retina. *The Journal of Comparative Neurology, 300*, 5–25.

Curcio, C. A., Sloan, K. R., Kalina, R. E., & Hendrickson, A. E. (1990b). Human photoreceptor topography. *The Journal of Comparative Neurology, 292*, 497–523.

Dacey, D. M., & Petersen, M. R. (1992). Dendritic field size and morphology of midget and parasol cells of the human retina. *Proceedings of the National Academy of Sciences of the United States of America, 89*, 9666–9671.

Dacey, D. M. (1993). The mosaic of midget ganglion cells in the human retina. *The Journal of Neuroscience, 13*, 5334–5355.

Derrington, A. M., & Lennie, P. (1984). Spatial and temporal contrast sensitivities of neurons in lateral geniculate nucleus of macaque. *The Journal of Physiology, 357*, 219–240.

Drasdo, N. (1977). The neural representation of visual space. *Nature, 266*, 554–556.

Drasdo, N., Millican, C. L., Katholi, C. R., & Curcio, C. A. (2007). The length of Henle fibers in the human retina and a model of ganglion receptive field density in the visual field. *Vision Research, 47*, 2901–2911.

Edgar, G. K., & Smith, A. T. (1990). Hemifield differences of perceived spatial frequency. *Perception, 19*, 759–766.

Fahle, M., & Schmid, M. (1988). Naso-temporal asymmetry of visual perception and of the visual cortex. *Vision Research, 28*, 293–300.

Fahle, M., & Wehrhahn, C. (1991). Motion perception in the peripheral visual field. *Graefe's Archive for Clinical and Experimental Ophthalmology, 229*, 430–436.

He, S., Cavanagh, P., & Intrilligator, J. (1996). Attentional resolution and the locus of visual awareness. *Nature, 383*, 334–337.

Hugdahl, K., & Davidson, R. J. (2003). *The Asymmetrical Brain*. Cambridge, MA: MIT Press, pp. 259–302.

Ivry, R. B., & Robertson, L. C. (1998). *The two sides of perception*. Cambridge, MA: MIT Press, pp. 41–45, 77–82.

Kryger, Z., Galli–Resta, L., Jacobs, G. H., & Reese, B. E. (1998). The topography of rod and cone photoreceptors in the retina of the ground squirrel. *Visual Neuroscience, 15*, 685–691.

Lee, B. B., Martin, P. R., Valberg, A., & Kremers, J. (1993). Physiological mechanisms underlying psychophysical sensitivity to combined luminance and chromatic luminance modulation. *Journal of the Optical Society of America A, 10*, 1403–1412.

Levi, D. M., Klein, S. A., & Aitsebaomo, A. P. (1985). Vernier acuity, crowding and cortical magnification. *Vision Research, 25*, 963–977.

Mackeben, M. (1999). Sustained focal attention and peripheral letter recognition. *Spatial Vision, 12*, 51–72.

Maddess, T., Goldberg, I., Wine, S., Dobinson, J., Welsh, A. H., & James, A. C. (1999). Testing for glaucoma with the spatial frequency doubling illusion. *Vision Research, 39*, 4258–4273.

Marmor, M. F., Hood, D. C., Keating, D., Kondo, M., Seeliger, M. W., & Miyake, Y. (2003). Guidelines for basic multifocal electroretinography (mfERG). *Documenta Ophthalmologica, 106*, 105–115.

Mendes, M., Silva, F., Simoes, L., Jorge, M., Saraiva, J., & Castelo-Branco, M. (2005). Visual magnocellular and structure from motion perceptual deficits in a neurodevelopmental model of dorsal stream function. *Brain Research. Cognitive Brain Research, 25*, 788–798.

Myerson, J., Manis, P. B., Miezin, F. M., & Allman, J. M. (1977). Magnification in striate cortex and retinal ganglion cell layer of owl monkey: A quantitative comparison. *Science, 198*, 855–857.

Nakayama, K., & Mackeben, M. (1989). Sustained and transient components of focal visual attention. *Vision Research, 29*, 1631–1646.

Østerberg, G. (1935). Topography of the layer of rods and cones in the human retina. *Acta Ophthalmologica, 13*, 1–103.

Packer, O., Hendrickson, A. E., & Curcio, C. A. (1989). Photoreceptor topography of the retina in the adult pigtail macaque (Macaca nemestrina). *The Journal of Comparative Neurology, 288*, 165–183.

Perry, V. H., & Cowey, A. (1985). The ganglion cell and cone distribution in the monkey retina: Implications for central magnification factors. *Vision Research, 25*, 1795–1810.

Previc, F. H. (1990). Functional specialization in the lower and upper visual fields in humans: Its ecological origins and neurophysiological implications. *The Behavioral and Brain Sciences, 13*, 519–575.

Rijsdijk, J. P., Kroon, J. N., & van der Wilt, G. J. (1980). Contrast sensitivity as a function of position on the retina. *Vision Research, 20*, 235–241.

Rolls, E. T., & Cowey, A. (1970). Topography of the retina and striate cortex and its relationship to visual acuity in rhesus monkeys and squirrel monkeys. *Experimental Brain Research, 10*, 298–310.

Rovamo, J., Virsu, V., & Nasanen, R. (1978). Cortical magnification factor predicts the photopic contrast sensitivity of peripheral vision. *Nature, 271*, 54–56.

Rovamo, J., & Virsu, V. (1979). An estimation and application of the human cortical magnification factor. *Experimental Brain Research, 37*, 495–510.

Rubin, N., Nakayama, K., & Shapley, R. (1996). Enhanced perception of illusory contours in the lower versus upper visual hemifields. *Science, 271*, 651–653.

Schein, S. J. (1988). Anatomy of macaque fovea and spatial densities of neurons in foveal representation. *The Journal of Comparative Neurology, 269*, 479–505.

Shapley, R., Kaplan, E., & Soodak, R. (1981). Spatial summation and contrast sensitivity of X and Y cells in the lateral geniculate nucleus of the macaque. *Nature, 292*, 543–545.

Silva, M. F., Faria, P., Regateiro, F. S., Forjaz, V., Januario, C., Freire, A., et al. (2005). Independent patterns of damage within magno-, parvo- and koniocellular pathways in Parkinson's disease. *Brain, 128*, 2260–2271.

Silveira, L. C., & Perry, V. H. (1991). The topography of magnocellular projecting ganglion cells (M-ganglion cells) in the primate retina. *Neuroscience, 40*, 217–237.

Silveira, L. C., Yamada, E. S., Perry, V. H., & Picanco–Diniz, C. W. (1994). M and P retinal ganglion cells of diurnal and nocturnal New–World monkeys. *Neuroreport, 5*, 2077–2081.

Thibos, L. N., Cheney, F. E., & Walsh, D. J. (1987). Retinal limits to the detection and resolution of gratings. *Journal of the Optical Society of America A, 4*, 1524–1529.

Van Essen, D. C., Newsome, W. T., & Maunsell, J. H. R. (1984). The visual field representation in striate cortex of the macaque monkey: Asymmetries, anisotropies, and individual variability. *Vision Research, 24*, 429–448.

Virsu, V., & Rovamo, J. (1979). Visual resolution, contrast sensitivity, and the cortical magnification factor. *Experimental Brain Research, 37*, 475–494.

Weymouth, F. W. (1958). Visual sensory units and the minimal angle of resolution. *American Journal of Ophthalmology, 46*, 102–113.

Wikler, K. C., & Rakic, P. (1990a). Distribution of photoreceptor subtypes in the retina of diurnal and nocturnal primates. *The Journal of Neuroscience, 10*, 3390–3401.

Wikler, K. C., Williams, R. W., & Rakic, P. (1990b). Photoreceptor mosaic: Number and distribution of rods and cones in the rhesus monkey retina. *The Journal of Comparative Neurology, 297*, 499–508.

Williams, D. R., & Coletta, N. J. (1987). Cone spacing and the visual resolution limit. *Journal of the Optical Society of America A, 4*, 1514–1523.

Yamada, E. S., Marshak, D. W., Silveira, L. C., & Casagrande, V. A. (1998). Morphology of P and M retinal ganglion cells of the bush baby. *Vision Research, 38*, 3345–3352.

Yamada, E. S., Silveira, L. C., Perry, V. H., & Franco, E. C. (2001). M and P retinal ganglion cells of the owl monkey: Morphology, size and photoreceptor convergence. *Vision Research, 41*, 119–131.